A measurement of parity-violating gamma-ray asymmetries in polarized cold neutron capture DRAFT

G.S. Mitchell [d], C.S. Blessinger [c], J.D. Bowman [d], T.E. Chupp [f], K.P. Coulter [f], M. Gericke [c], G.L. Jones [b], M.B. Leuschner [g], H. Nann [c], S.A. Page [e], S.I. Penttilä [d], T.B. Smith [a], W.M. Snow [c], W.S. Wilburn [d]

[a] *University of Dayton, Dayton, OH 45469, USA*

[b] *Hamilton College, Clinton, NY 13323, USA*

[c] *Indiana University, Bloomington, Indiana 47405, USA*

[d] *Los Alamos National Laboratory, Los Alamos, New Mexico 87545, USA*

[e] *University of Manitoba, Winnipeg, Manitoba R3T 2N2, Canada*

[f] *University of Michigan, Ann Arbor, Michigan 48104, USA*

[g] *University of New Hampshire, Durham, New Hampshire 03824, USA*

Abstract

An apparatus for measuring parity-violating asymmetries in gamma-ray emission following polarized cold neutron capture was constructed as a 1/10th scale test of the design for the forthcoming $\vec{n} + p \rightarrow d + \gamma$ experiment at LANSCE. The elements of the polarized neutron beam, including a polarized ^{3}He neutron spin filter and radio frequency neutron spin rotator, are described. Using CsI(Tl) detectors and photodiode current mode readout, measurements were made of asymmetries in gamma-ray emission following neutron capture on ^{35}Cl, ^{139}La, and ^{113}Cd targets. Parity-violating asymmetries were observed with ^{35}Cl and ^{139}La, and no statistically significant ($> 6 \times 10^{-6}$) parity-allowed asymmetries were seen.

Key words: parity violation, polarized neutrons, radiative neutron capture
PACS: 11.30.Er, 13.75.Cs, 07.85.-m, 25.40.Lw

1 Introduction

The NPDGamma experiment [1,2] is under construction at the Los Alamos Neutron Science Center (LANSCE) at Los Alamos National Laboratory. This

includes construction of Flight Path 12 at the Manuel Lujan Jr. Neutron Scattering Center at LANSCE, which will be a pulsed cold neutron beamline dedicated to fundamental physics. The goal of the experiment is to measure the parity-violating directional gamma asymmetry A_γ in the reaction $\vec{n} + p \rightarrow d + \gamma$ to an accuracy of 5×10^{-9}, which is approximately 10% of its predicted value [3]. This measurement will provide a theoretically clean measurement of the weak pion-nucleon coupling and resolve the long-standing controversy over its value [4,5]. The experiment will consist of a pulsed, cold neutron beam, transversely polarized by transmission through polarized ^{3}He, incident on a liquid para-hydrogen target. The 2.2 MeV gammas from the capture reaction will be detected by an array of CsI(Tl) scintillators coupled to vacuum photodiodes and operated in current mode. In Fall 2000, an engineering run using prototypes of all major components to measure parity-violating asymmetries in neutron capture on several nuclei was completed. Uncertainties of order 6×10^{-6}, limited by counting statistics, were obtained after several hours of running using Cl, Cd, and La capture targets. This paper will discuss the results of this engineering run and the status of the NPDGamma experiment.

Parity-violating asymmetries such as A_γ in the $\vec{n} + p \rightarrow d + \gamma$ capture gamma flux (which follows $1 + A_\gamma \cos\theta$, where θ is the angle between the neutron polarization and photon momentum) arise due to weak interactions, which allow mixing and interference between transitions from opposite parity states. For example, in $\vec{n} + p \rightarrow d + \gamma$ weak effects allow a small amount of E1 transition to interfere with the primary M1 amplitude. In systems with $Z > 1$ the interference may be more complicated, involving many states and many transitions. Previous measurements of parity violation following polarized cold neutron capture include [6,7]. Parity-allowed asymmetries in the gamma emission following neutron capture are also possible [8]. It is possible that a significant parity-allowed asymmetry in gamma emission following polarized cold neutron capture may exist with a ^{35}Cl or ^{139}La target nucleus.

The motivation for measuring parity-violating and parity-allowed asymmetries on Cl, La, and Cd targets was two-fold: to test a 1/10th scale apparatus at the few $\times 10^{-6}$ level, and to look for a large parity-allowed asymmetry which would be useful for a detector alignment scheme for the NPDGamma experiment. Other goals of this engineering run were to gain knowledge of the neutron source moderator brightness and to measure intensity fluctuations in the neutron beam.

2 Description of Setup

This section describes the apparatus used in Fall 2000 to measure directional asymmetries in gamma-ray emission following polarized cold neutron capture on nuclear targets. A schematic picture of the setup is shown in Fig. 1.

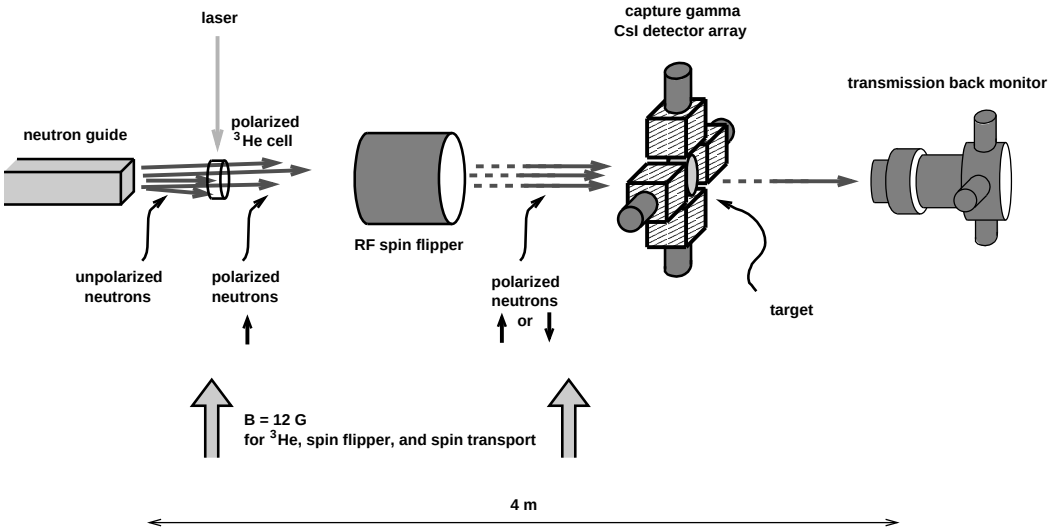

Fig. 1. Experimental setup for asymmetry measurements on nuclear targets. Various elements of collimation and shielding and the large coils providing the vertical ∼12 G field are not shown. The magnetic field covered the region from the end of the guide to the target.

2.1 Pulsed Cold Neutron Beam

The LANSCE linear accelerator provides 800 MeV protons to a proton storage ring, which after compression of the beam delivers 250 ns wide pulses at 20 Hz to a split tungsten spallation target. The target is surrounded by several moderators, including a partially coupled cold hydrogen moderator viewed by Flight Path 11A (FP11A). The performance of the moderator is modeled in [9]. The neutron flux is directed through FP11A by a ^{58}Ni-coated 6×6 cm^2 guide which begins 1 m from the moderator and is 18.5 m long. On the scale of 50 ms between pulses, the proton pulse width is very short. An experiment located ∼20 m from the source will see a time of flight spectrum of cold neutrons: for the typical energies of interest (1-100 meV, 1-9 Å) neutrons will arrive 4.5-45 ms after the proton pulse. Knowledge of time of flight (tof) and the flight path length determines the neutron energy.

2.2 Measurement of Cold Neutron Flux

An absolute measurement of the cold neutron flux was made by tightly collimating the beam with a 4 mm diameter Gd foil collimator. The collimator was placed 15 cm from the end of the guide. A 4.1 mm diameter ^{6}Li-loaded glass scintillator was mounted on a photomultiplier tube which was itself mounted in an x-y positioner. This detector was located 2.65 m from the end of the guide. The collimation reduced the neutron rate enough to permit normal pulse counting techniques (to less than 60 kHz for energies less than 15 meV). With incident proton current of 90 μA, the peak neutron flux out of the end of the uncollimated FP11A guide was 1.4×10^6 neutrons/ms per pulse at 8 meV, and the total flux from 2.5 to 40 meV was 2.5×10^7 neutrons per pulse. Using the geometry of the flight path and the collimation to convert from the measured rates, the result was a measured moderator brightness of 20% lower than predicted by [9] for energies 1-15 meV. The flux will be sufficient for the full NPDGamma experiment to make a raw asymmetry measurement of 1×10^{-4} per neutron pulse and to have the planned run time of three six month run cycles, where a run cycle consists of 2500 hours of 150 μA proton beam.

2.3 Intensity Fluctuations

Density fluctuations in the moderator could effectively produce pulse-to-pulse position fluctuations of the beam larger than the counting statistics of the experiment. A simple Monte Carlo study of intensity-induced position fluctuations of the neutron beam produced the result that intensity fluctuations with a variance less than $\sigma^2 \approx 10^{-4}$ are acceptable. Three sets of measurements were made of correlations between a proton current toroid monitor and a ^{3}He ion chamber neutron flux monitor. The neutron intensity fluctuations for constant incident proton current were $\sigma^2 \approx 10^{-5}$ for each set of measurements, an order of magnitude better than the requirement. These measurements of the intensity fluctuations of the beam for constant proton current incident on the spallation target show that density fluctuations or bubbles in the liquid hydrogen moderator were not a problem for the asymmetry measurements in this engineering run, and they will not be a problem for NPDGamma.

2.4 ^{3}He Spin Filter

Cold neutron beams can be polarized in several ways, but the best technology for NPDGamma is a ^{3}He spin filter [10]. This allows for a polarizer which can have a large acceptance angle and area, while itself requiring little space. In contrast to a polarizing supermirror, a ^{3}He spin filter does not require a strong

magnetic fields or produce field gradients, which are important benefits for control of systematic errors in NPDGamma. For this engineering run a system with a double-chambered glass cell was used to contain the ^{3}He. The cell also contained a small amount of Rb and N_2 as well. The ^{3}He was polarized by spin-exchange optical pumping. The polarization of the ^{3}He proceeds by optically pumping the 795 nm $5s - 5p$ transition for the Rb valence electron, which transfers its spin to the ^{3}He nucleus by a hyperfine interaction upon collision. The cross-section for cold neutron absorption by ^{3}He is essentially zero for parallel neutron and nuclear spins, but due to a large spin zero resonance in ^{4}He, there is a large absorption cross-section for anti-parallel spins. Thus a polarized volume of ^{3}He can filter out one spin state of an unpolarized neutron beam and produce large neutron polarizations. The thickness of the spin filter can be optimized for polarization versus transmission.

A $\sim$12 G holding field is used to provide a uniform field parallel to the polarization direction and to prevent depolarization of the ^{3}He by magnetic field gradients. Circularly polarized 795 nm laser light for electronic polarization of the Rb was provided by two 15 W laser diode arrays. One chamber of the cell, the pumping chamber, was in a small oven which was kept at 175 °C to produce Rb vapor, and this part was illuminated by the diode lasers; the other part of the cell, the polarizer, was the volume placed in the neutron beam and used to filter out the undesired polarization state. The polarizer chamber as seen by the neutron beam was circular, 7 cm in diameter, and 1.6 cm thick. Both upstream and downstream surfaces were concave with respect to the beam direction, in order to provide a uniform cell length to the beam while maintaining curved surfaces to prevent cell explosion. The polarizer chamber was connected by a 1 cm long glass feedthrough tube to the roughly spherical and $\sim$6 cm diameter pumping chamber. The absolute neutron polarization was measured using a supermirror [12] and an ion chamber back monitor (discussed below), and reversing the ^{3}He polarization direction using an NMR adiabatic fast passage spin flip. Relative ^{3}He polarizations were measured during data taking by an NMR pickup coil system.

Neutron polarization varied from $P = 0.3$ to 0.7 for neutron energies of 10 meV to 2 meV, shown in Fig. 2. The neutron polarization is given by $P_n = \tanh(n_3 \sigma L P_3)$ where n_3 is the number density of ^{3}He, $\sigma = (26.8/\sqrt{E})$ kb, E is neutron energy in meV, L is the length of the polarizer volume, and P_3 is the ^{3}He polarization. At typical operating temperature, the 6.0 atm cm polarizer section of this cell had ^{3}He polarization of $P_3 = 0.265$. The relative error on the neutron polarization is 2%, a combination of three roughly equal sources of error. These are: knowledge of the supermirror analyzing power, absolute scale of the NMR system, and statistical spread of individual NMR measurements.

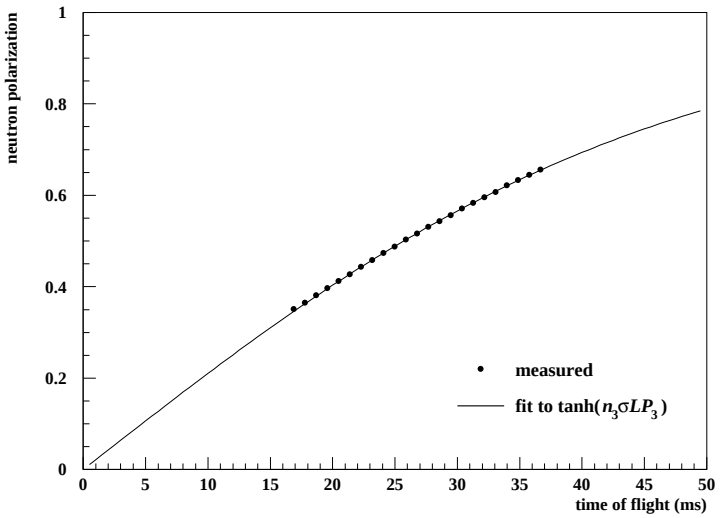

Fig. 2. Neutron polarization. Measured points were obtained using a supermirror and ion chamber to compare neutron transmission of opposite ^{3}He polarization directions. The curve is a fit to $P_n = \tanh(n_3\sigma L P_3)$, with P_3 as a fitted parameter, using $n_3 L = 6.0$ atm cm for the thickness of the ^{3}He cell. The flight path length to the ^{3}He cell was 21.08 m. The flight path length to the back monitor was 23 m, which is used here to relate the time of flight to neutron energy and σ, the ^{3}He cross-section.

2.5 Spin Flipper

To isolate a small parity-violating asymmetry, a common technique is to reverse the polarization of the incident beam and observe a coherent change in the reaction products. For NPDGamma and for this test run, the neutron spins are flipped on a 20 Hz pulse-by-pulse basis with a radio frequency spin flipper (RFSF). The RFSF is a shielded solenoid, 30 cm in diameter and 30 cm long, with the aluminum shielding canister a total of 10 cm larger in each dimension. The windows encountered by the neutron beam are 2 mm thick. The RFSF is similar to that employed in [11] with two modifications: the aluminum shielding, and the amplitude of the RF field is ramped down with an inverse time dependence every pulse to match the time the neutrons spend traversing the length of the coil. This provides efficient pulse-to-pulse control of neutron polarization state for a wide range of energies, without introducing significant static magnetic fields or gradients into the rest of the apparatus.

The spin flipper RF field amplitude and frequency were tuned using the polarized neutron beam produced by the ^{3}He system and a supermirror [12] to analyze the flipped pulses. The ^{3}He/H_2 ion chamber back monitor was placed downstream of the supermirror and the difference it recorded between RFSF on and off pulses yielded the RFSF efficiency. The RFSF was typically driven at 34 kHz in the holding field of 12 G, a relationship determined by the neutron gyromagnetic ratio $\gamma = -2.916 \times 10^7$ Hz/T. For a 2.5 cm collimated beam, the

RFSF efficiency, defined as the absolute ratio of transmitted (flipped) neutron polarization to incident polarization, was measured to be $\epsilon = 0.98 \pm 0.02$. This efficiency is sufficiently large and well-known for NPDGamma.

2.6 Beam Monitors

Two beam monitors were used in this test run: a front monitor with ^{3}He and ^{4}He, and a back monitor with ^{3}He and H_2. As discussed above, the front monitor was used to measure fluctuations in beam intensity. It was then removed from the beamline. The back monitor, which was similar in design to [13], was used to study the ^{3}He spin filter system and the RFSF. Its chamber contained a gas mix of 0.5 atm ^{3}He and 3 atm H_2. The chamber housed ten 7.6 cm diameter, 0.76 mm thick Al collection plates spaced evenly by 2.5 cm increments along the beam axis, and ten electrodes held at 3 kV. The signals from the collection plates were read out to current to voltage amplifiers, each with a 100 MΩ gain resistor.

2.7 Nuclear Targets

For parity-violating and parity-allowed asymmetry measurements, three targets were used. As a chlorine target, an aluminum canister was filled with CCl_4 (natural Cl). The CCl_4 thickness seen by the neutron beam was 3.8 cm. As a lanthanum target, a natural La (99.91% ^{139}La) metal cylinder 10.2 cm in diameter and 2.5 cm thick was housed in a 1 mm thick stainless steel can. As a cadmium target, a 0.76 mm thick piece of natural Cd metal was cut into a 10.2 cm diameter circle. To eliminate neutron backgrounds and reduce activation of the CsI(Tl), the targets were in turn mounted in a cylinder of ^{6}Li-doped plastic with inner diameter 10.2 cm and outer diameter 15.2 cm. The neutron beam was collimated to 5 cm diameter and no neutrons were directly incident on the plastic cylinder. The targets were located at a flight path length of 21.9 m.

2.8 Gamma-ray Detectors

To detect the gammas emitted following neutron capture, an array of four CsI(Tl) crystals was symmetrically mounted around the target volume. The crystals are housed in Al canisters with external dimensions $15 \times 16.5 \times 16.5$ cm^3. The closest faces of the detectors were 8.4 cm from the central axis of the neutron beam. The crystals were viewed with 70 mm vacuum photodiodes (Hamamatsu R2046PT), biased at -90 V. The photoelectron yield of the

crystals was measured to be ∼500 p.e./MeV, and typical photodiode currents were a few nA. The magnetic field sensitivity of the photodiode signals was measured to be less than 1×10^{-4}/G in a 10 G field directed perpendicular to the photodiode axis.

The current signals from the photodiodes were read out into a low-noise solid state current to voltage preamplifier with a gain resistor of 10 MΩ. With the neutron beam off, the r.m.s. noise per sample was measured to be of order 1 mV. The preamplifier signals were sampled at 25 kHz with 16 bit ADC's in a VME system, and the data compressed by a factor of ten to be written as 100 samples over 40 ms per pulse. Pedestal values for the detectors were typically 100 ADC counts, or 30 mV. An average gamma-ray intensity spectrum, indicative of the time structure of the neutron flux, is shown in Fig. 3.

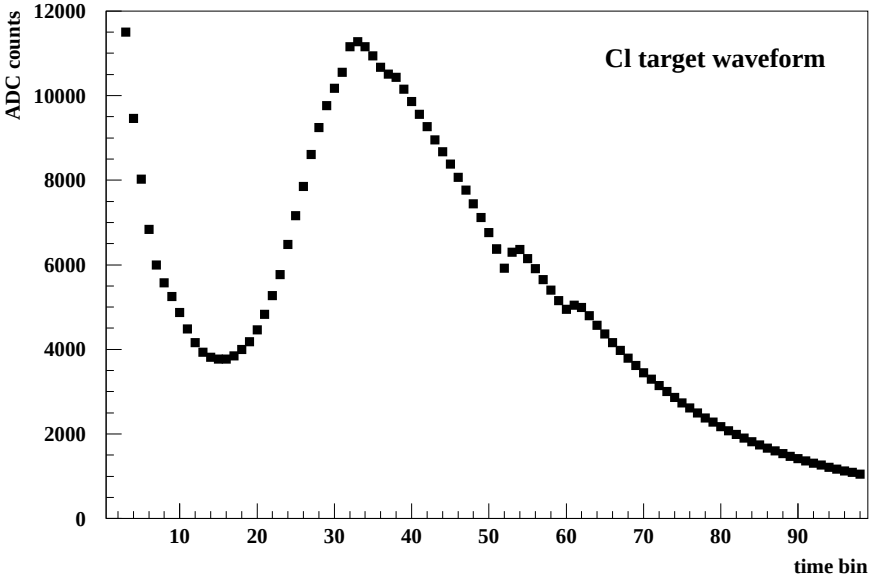

Fig. 3. Average spectrum for a Cl target run. The x axis of time bins 0-100 corresponds to time of flight of 0-40 ms. The y axis of ADC counts is proportional to the voltage signal out of the preamplifier, where one ADC count is 0.3 mV. The dips in the spectrum at time bins greater than 35 are due to Bragg edges of materials such as aluminum windows in the flight path.

3 Asymmetry Measurements

Asymmetry measurements were made on three targets. The neutron energy range analyzed in each case was 2.5 meV to 40 meV, corresponding to 8-32 ms time of flight, or 1.4-5.7 Å.

Asymmetries were formed using matched eight-step spin sequences (↑↓↓↑↓↑↑↓) of consecutive pulses and a calculation of the geometric mean asymmetry

within the sequence. The raw experimental asymmetries are calculated as follows:

$$A_{\rm raw} = \frac{\sqrt{\frac{U_\uparrow D_\downarrow}{U_\downarrow D_\uparrow}} - 1}{\sqrt{\frac{U_\uparrow D_\downarrow}{U_\downarrow D_\uparrow}} + 1}$$

where U, D refer to the upper and lower detector, and the subscripts $\uparrow, \downarrow$ refer to the neutron spin direction. The state $\uparrow$ corresponds to spin flipper on, $\downarrow$ to spin flipper off. The asymmetry $A_{\rm raw}$ was calculated for each valid eight-step spin sequence, in each case four steps added together to obtain $U_\uparrow$ and $D_\uparrow$ and the other four to obtain $U_\downarrow$ and $D_\downarrow$. For each step the detector signals were summed over the data from the 20th to 80th of the 100 samples. This range in time of flight corresponds to the peak of the neutron distribution, and to a region of well-understood neutron polarization and spin flipper efficiency. An identical procedure was used for the left and right detector pair. A cut was made to eliminate sequences which had pulses with anomalous incident neutron fluxes. If any of the eight steps had a detector sum $(U + D + L + R)$ that differed by more than 1% from the average of all the sequences in the sum, the entire eight-step sequence was discarded. This cut removed less than 1% of the data. The final data set for each target consisted of 6.5 to 8.4×10^4 eight-step sequences.

The sets of eight-step asymmetries were histogrammed and fit by minimizing χ^2 compared to a Gaussian distribution to extract the mean value and the error in the mean. A histogram of ^{35}Cl asymmetry values is shown in Fig. 4. The histograms consisted of 6000 bins covering the range $[-0.003, 0.003]$, to allow sufficient precision in the fits. No asymmetry values fell outside the limits of the histograms. The results of the fitting are consistent with a simple average of each data set, but fitting is used to provide a more robust result in the case of a few outlier eight-step values. The signs of the asymmetries were carefully checked through the data acquisition electronics and analysis code.

Parity-violating asymmetries were detected (greater than two standard deviations from zero) in neutron capture on the Cl and La targets. No parity-allowed asymmetry was seen in those targets. No asymmetry of either type was observed with the Cd target. Results are presented in Table 1.

The measured asymmetries $A_{\rm raw}$ were corrected to physics asymmetries using

$$A_\gamma = \frac{(A_{\rm raw} - A_{\rm noise})}{RPTG}$$

where $A_{\rm noise}$ is a measured false asymmetry due to electronic noise pickup, R is the spin flipper efficiency, P is the neutron polarization, T is a factor for neutron depolarization in the target prior to capture, and G is a geometry factor for the average angle of the gamma rays seen by the detectors relative

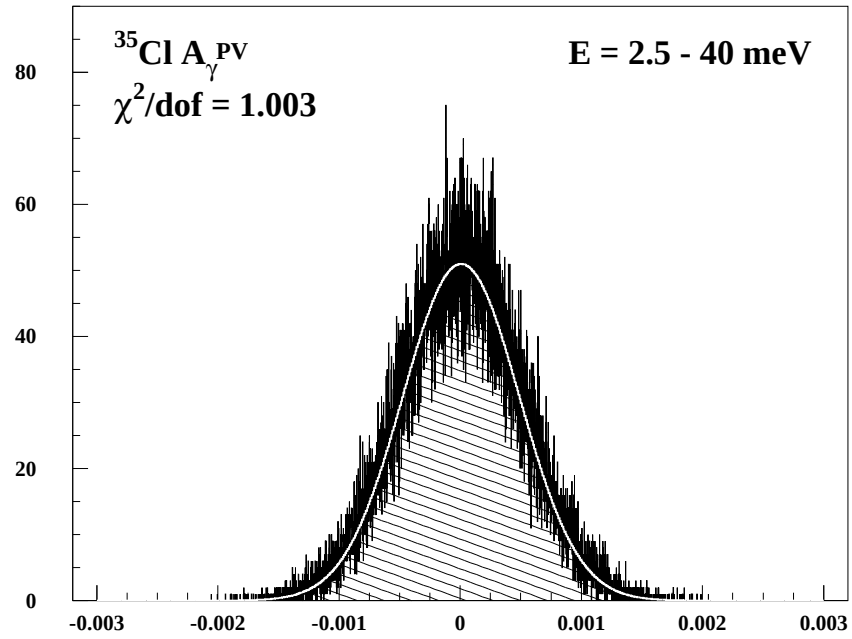

Fig. 4. Histogram of asymmetry values from eight-step sequences for the Cl target. The mean and error in the mean are determined from a fit to a Gaussian distribution, as shown.

Raw Asymmetries $\times 10^{-6}$

	PV	PA
^{35}Cl	-7.5 ± 1.9	-3.1 ± 1.9
^{113}Cd	$+0.4 \pm 1.4$	-2.5 ± 1.4
^{139}La	-5.3 ± 1.9	$+0.0 \pm 1.9$

Parity-allowed (left-right) $\times 10^{-6}$

	^{35}Cl	^{113}Cd	^{139}La
this work	-10.6 ± 6.5	-7.9 ± 4.4	$+0.0 \pm 6.1$

Parity-violating (up-down) $\times 10^{-6}$

	^{35}Cl	^{113}Cd	^{139}La
Leningrad [6]	-27.8 ± 4.9	-1.3 ± 1.4	-17.8 ± 2.2
ILL [7]	-21.2 ± 1.7	-	-
this work	-25.7 ± 6.5	$+1.3 \pm 4.4$	-17.0 ± 6.1

Table 1
Results. Given errors are statistical only, as systematic errors are less than 10%. (PV is $s_n \cdot k_\gamma$, PA is $s_n \cdot (k_\gamma \times k_n)$, where s_n is the neutron spin direction, k_n is the neutron momentum vector, and k_γ is the photon momentum vector.)

to the neutron polarization. These factors are discussed in the following five paragraphs.

The electronic noise asymmetry was measured before and after the neutron capture data were acquired. With no neutrons incident on the apparatus, the

average of two one-hour runs was $A_{\rm noise}^{UD} = (0.12 \pm 0.26) \times 10^{-6}$ and $A_{\rm noise}^{LR} = (0.42 \pm 0.25) \times 10^{-6}$. These values were extracted from the data using the same method as for $A_{\rm raw}$. Since these values are less than two standard deviations from zero and are an order of magnitude smaller than the statistical error, $A_{\rm noise} = 0$ is used to obtain physics asymmetries from the raw asymmetries.

Since the RFSF is on for half the neutron pulses, the measured spin flipper efficiency $\epsilon = 0.98 \pm 0.02$ yields a factor of $R = (1 + \epsilon)/2 = 0.99 \pm 0.01$ for converting to a physics asymmetry.

The absolute neutron polarization was measured using the supermirror analyzer and back monitor neutron detector, and fit to a hyperbolic tangent function to relate the pickup coil NMR signal to P_3. NMR measurements were made during data taking and the NMR signal amplitudes measured during data taking with each target were used to provide a P_3 for the hyperbolic tangent expression given earlier for neutron polarization versus energy. The convolution of the neutron polarization values and the detector signals (versus energy) leads to factors of $P = 0.37, 0.37, 0.38$ for the Cl, Cd, and La targets respectively.

Neutron depolarization in the target, T, is accounted for using cross-section values for (n,γ), spin-coherent scattering, and spin-incoherent scattering, taken from [14]. A simple Monte Carlo was written to propagate neutrons through the target material according to the cross-sections (assuming a $1/v$ dependence of the capture cross-section for ^{35}Cl and ^{139}La), and upon each scattering event the probability of spin-flip scattering was accounted for by taking the ratio of $\frac{2}{3}$ of the spin-incoherent scattering cross-section to the total scattering cross-section. Depolarization was determined by computing an average value for $(-1)^n$ where n was the number of spin-flip scatterings prior to capture. The convolution of the depolarization values with the detector signals leads to factors of $T = 0.92, 1.00, 0.94$ for Cl, Cd, and La respectively. For each target, it was assumed that isotopes other than the one of interest (^{35}Cl, ^{113}Cd, and ^{139}La) contribute negligibly to the scattering, capture, or A_γ.

The geometrical acceptance of the detector crystals was modeled using the computer code MCNP [15]. The result for average $\cos(\theta)$ for parity-violating (up-down) asymmetry and for average $\sin(\theta)$ for the parity-allowed (left-right) asymmetry yielded factors of $G = 0.86, 0.86, 0.87$ for Cl, Cd, and La respectively. The angle θ is that between the neutron polarization axis and the gamma ray momentum.

The statistical errors on the asymmetries follow the expectation of counting statistics given the measured neutron flux. Systematic errors are small on the correction factors discussed above: 1% on R, 2% on P, 2% on T, and 5% on G. Studies which split the data into independent sets to compare asymmetry

results discovered no anomalous effects.

A theoretical estimation of a parity violating effect in polarized cold neutron capture on ^{35}Cl yielded the result $A_\gamma = -(37 \pm 18) \times 10^{-6}$ [16], which is consistent with these results in both sign and magnitude.

4 Summary and Prospects

The parity-violating neutron capture asymmetry measurements reported here are consistent with previous experimental results [6,7] and of comparable precision. However, they were made in a fraction of the run time (eight hours per target) due to the large flux available with the pulsed beamline at LANSCE.

The parity violation in neutron capture on Cl and La is more than an order of magnitude larger than a naive estimate for the size of the effect: $G_F\, k_F^2 \approx (1.17 \times 10^{-5}\,\mathrm{GeV}^{-2})(0.2\,\mathrm{GeV})^2 \approx 5 \times 10^{-7}$, where G_F is the Fermi weak coupling constant and k_F is the momentum typical of a nucleon in a nucleus. This enhancement is interpreted in terms of two factors: dynamic enhancement, which is due to close spacing of two levels of opposite parity; and kinematic enhancement, which is due to the widths of the states involved. Even for a system with well-known low-lying states such as the compound nucleus ^{36}Cl, detailed and accurate calculations of these effects are not easily done. Interpretation of parity violation measurements in many-body systems in terms of a simple hadronic weak interaction is difficult. A clean theoretical picture only presents itself for few-nucleon systems such as $n-p$ interactions.

No parity-allowed asymmetries were seen in these measurements, at the level of 10^{-6}. A large parity-allowed asymmetry would provide a useful technique for alignment of the NPDGamma detector array by observing the mixing of the known left-right asymmetry into the up-down detector channels. Another possible method to measure the angle of each detector element to 20 mrad precision would be to scan a small neutron capture target in x-y and observe the change in detected gamma intensity. However, to remove the variable of beam nonuniformity, a method using translation of the array (rather than translation of a capture target) will be used for the full NPDGamma experiment.

This engineering run, as compared to the full apparatus that will be constructed for the NPDGamma experiment, was missing the following components: a frame overlap chopper, a full-sized ^{3}He system, a liquid para-hydrogen target, and a full complement of detectors. A new beamline at LANSCE for nuclear physics is under construction with a larger (9.5×9.5 cm^2 vs. 6×6 cm^2) $m = 3$ supermirror guide. Scaling of the engineering run errors by run time,

proton current, moderator brightness, guide characteristics of size and trasmission, and detector solid angle, yields an expected statistical error on $A_{\rm raw}$ for $\overrightarrow{n} + p \rightarrow d + \gamma$ of 0.5×10^{-8} in 7500 hours of delivered neutron beam, or three years of LANSCE run cycles. All tests show that the experimental design and method are sufficient to make a measurement of this precision for NPDGamma.

References

[1] Snow, W. M., et al., Nucl. Instr. and Meth. A440, 729 (2000).

[2] Snow, W. M., et al., `http://arXiv.org/nucl-ex/9804001`.

[3] Desplanques, B., et al., Ann. Phys. 124, 449 (1980).

[4] Adelberger, E. G., and Haxton, W. C., Annu. Rev. Nucl. Part. Sci. 35, 501 (1985).

[5] Haeberli, W., and Holstein, B. R., in *Symmetries and Fundamental Interactions in Nuclei*, edited by Haxton, W.C., and Henley, E.M. (World Scientific, Singapore, 1995), pp. 17-66.

[6] Vesna, V. A., et al., JETP Lett. 36, 209 (1982).

[7] Avenier, M., et al., Nucl. Phys. A436, 83 (1985).

[8] Csoto, A., Gibson, B. F., and Payne, G. L., Phys. Rev. C56, 631 (1997).

[9] Ferguson, P. D., Russell, G. J., and Pitcher, E. J., 'Reference Moderator Calculated Performance for the LANSCE Upgrade Project,' ICANS-XIII (1995), PSI Report 95-02.

Also:

Muhrer, G., Ferguson, P. D., Russell, G. J., and Pitcher, E. J., 'As-Built Monte Carlo Model of the Lujan Target System and Comparison of its Neutronic Performance to a Physics Model,' LANL Report LA-UR-00-6078 (2000).

Donahue, J. B., et al., 'LANSCE Short-Pulse Spallation Source Target Upgrade,' Proceedings of the 1997 Particle Accelerator Conference Vancouver, BC, Canada, May 12-16, 1997, 1:190-192, Piscataway, NJ: IEEE, 1998.

[10] Jones, G. L., et al., Nucl. Instr. and Meth. A440, 772 (2000).

Rich, D. R., et al., Nucl. Instr. and Meth. A481, 431 (2002).

[11] Alvarez, L. W., and Bloch, F., Phys. Rev 57, 11 (1940).

[12] Schaerpf, O., Physica B 156 & 157, 631 (1989).

Schaerpf, O., Physica B 156 & 157, 639 (1989).

[13] Penn, S. D., et al., Nucl. Instr. and Meth. A457, 332 (2001).

[14] Sears, V. F., Neutron News 3, 29 (1992). Table available at: http://www.ncnr.nist.gov/resources/n-lengths/list.html.

[15] Code available from Radiation Safety Information Computational Center, Oak Ridge National Laboratory, as code package CCC-701 and data library DLC-200. See http://www-rsicc.ornl.gov/rsic.html.

[16] Bunakov, V. E., et al., Sov. J. Nucl. Phys. 40, 119 (1984). [Yad. Fiz. 40, 188 (1984).]